Available online at www.sciencedirect.com

SciVerse ScienceDirect

Ceramics International 39 (2013) 4063–4067

CERAMICS INTERNATIONAL

www.elsevier.com/locate/ceramint

Eu^{3+} luminescence in novel garnet-type $Li_5La_3Nb_2O_{12}$ ceramics

Xinmin Zhang[a], Fangui Meng[a], Hong Wei[a], Hyo Jin Seo[b,*]

[a]*College of Materials Science and Engineering, Central South University of Forestry and Technology, Changsha 410004, China*
[b]*Department of Physics, Pukyong National University, 599-1, Daeyeon 3-Dong, Nam-Gu, Busan 608-737, Republic of Korea*

Received 26 August 2012; received in revised form 24 October 2012; accepted 28 October 2012
Available online 5 November 2012

Abstract

A novel $Li_5La_3Nb_2O_{12}$:Eu^{3+} phosphor was synthesized by the solid-state reaction at high temperature. The phase purity of products was checked by XRD. The emission spectrum is independent of the excitation wavelength and the $^5D_0$–$^7F_2$ transition is the dominant one. In the excitation spectrum, there are some sharp peaks originating from the f–f transitions of Eu^{3+} and a broad band peaking at about 280 nm. The concentration dependence of emission intensity and decay curves of $^5D_0$–$^7F_2$ transition were investigated. The temperature dependence of emission intensity and decay curves were also investigated in detail.

Keywords: A. Powder: solid state reaction; C. Optical properties; D. Niobates

1. Introduction

Rare earth ions activated luminescence materials have grown considerably in recent years due to their excellent optical properties and their wide applications in the fields of lighting, display, medical diagnosis and so on [1–7]. It is well established that Eu^{3+} activated phosphors emit in the 580–625 nm spectral range depending on the local environment of Eu^{3+}. Recently, Eu^{3+} activated luminescent materials have been paid more attention as interesting candidates for potential red-emitting phosphors in white light-emitting diodes (white LEDs) [8]. White LEDs using blue chip combined with yellow phosphor ($Y_3Al_5O_{12}$:Ce^{3+}), although this phosphor exhibits high luminescence efficiency and chemical stability, show a lower color rendering index (CRI) due to the lack of red color contribution. In order to overcome this shortcoming, red phosphor is added for white LEDs having high CRI [9–11]. So it is important for developing new red phosphors to promote the development of high quality white LEDs.

Garnet-type compounds are a large family and their luminescence properties have been investigated widely [12–15]. Among them, YAG:Ce is one of the most famous phosphors [16]. $Li_5La_3Nb_2O_{12}$ is also a compound having garnet structure [17]. Many authors have reported the mechanism of Li ion transport in this crystal because of its potential application in Li-ion batteries. To the best of our knowledge, there are no reports concerning the Eu^{3+} luminescence in $Li_5La_3Nb_2O_{12}$ host. For the synthesis of rare earth ions activated luminescence materials, substitution occurs readily when two or more elements, with similar ionic radii and the same charge can take each other place within a crystal structure without substantially altering the crystal structure. In this case, La^{3+} is the component element in this host. So the La^{3+} ions could be very easy to be substituted by other rare earth ions due to similar ionic radii and the same charge. Hence we think it is worthwhile to investigate the luminescence properties of Eu^{3+} in $Li_5La_3Nb_2O_{12}$ host. In this paper, we synthesized a series of $Li_5La_3Nb_2O_{12}$:Eu^{3+} phosphors with different Eu^{3+} concentrations. Their luminescence properties were characterized by emission spectrum (room and high temperatures), excitation spectrum and luminescence decay behavior in detail.

2. Experimental

$Li_5(La_{3-x}Eu_x)Nb_2O_{12}$ phosphors were prepared by conventional solid-state reaction at high temperature. Raw materials Li_2CO_3 (excess 20 mol% to compensate the

---

*Corresponding author. Tel.: +82 51 629 5568; fax: +82 51 629 5549.
E-mail address: hjseo@pknu.ac.kr (H.J. Seo).

0272-8842/$ - see front matter © 2012 Elsevier Ltd and Techna Group S.r.l. All rights reserved.
http://dx.doi.org/10.1016/j.ceramint.2012.10.259

evaporation), La_2O_3, Eu_2O_3, and Nb_2O_5 (all materials are bought from Aldrich, 99.99%) were thoroughly mixed, and sintered in air at 900 °C for 24 h. X-ray powder diffraction (Beijing Puxi, XD-2, Cu Kα, $\lambda = 1.5405$ Å) was used to identify the structure of the final products. Excitation and emission spectra at room temperature were carried out by a fluorescence meter (Shimadzu, RF 5301PC) with a 150 W Xe lamp as an excitation source. The emission spectra and decay curves at the temperature range between 297 and 503 K were recorded by a 500 MHz digital storage oscilloscope (LeCroy 9350 A) in which the signal was fed from PMT. The samples were excited by 266 nm UV laser. The setup was equipped with a home-made heating cell connected to the temperature controller.

3. Results and discussion

As one of the garnet-type compounds, $Li_5La_3Nb_2O_{12}$ has a cubic unit cell with space group $I2_13$ (no. 199); the lattice parameters are $a = 12.797$ Å and $V = 2095.68$ Å^3 [17]. In order to check the phase purity of the samples, XRD measurement was carried out for all samples. The selected XRD patterns of $Li_5(La_{3-x}Eu_x)Nb_2O_{12}$ samples ($x = 0.02$, 0.15, 0.30, 0.50 and 1.0) are shown in Fig. 1. It is found that all observed diffraction peaks can be indexed to the standard date of $Li_5La_3Nb_2O_{12}$. No other impurity phases can be detected when Eu^{3+} ions are doped into the host lattice, indicating that the samples are of single phase. However, the XRD patterns are not consistent with the standard diffraction peaks of $Li_5La_3Nb_2O_{12}$ when the value of x is greater than 1.0. The heavy dopant products should have different crystal structures, which could be attributed to the radius difference of Eu^{3+} and La^{3+} ions. The crystal structure of these samples is under investigation.

The Eu^{3+} activated $Li_5La_3Nb_2O_{12}$ samples emit intense red luminescence under UV excitation (254 nm). It is found that the emission spectrum is independent of the excitation wavelength except for the emission intensity.

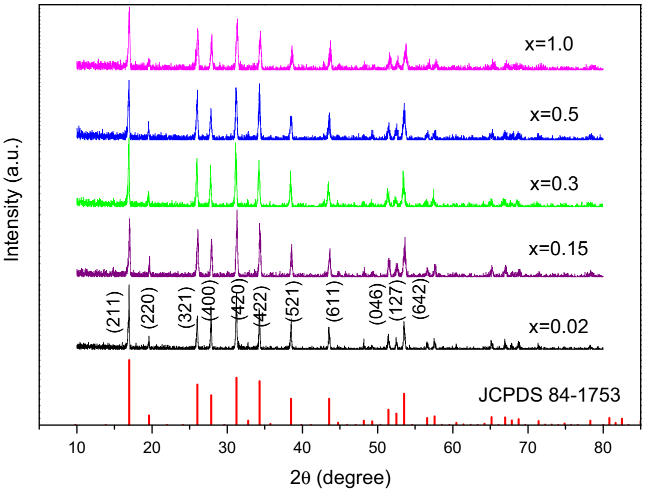

Fig. 1. XRD patterns of $Li_5(La_{3-x}Eu_x)Nb_2O_{12}$ samples. Standard data for $Li_5La_3Nb_2O_{12}$ (JCPDS card no. 84–1753) is shown as a reference.

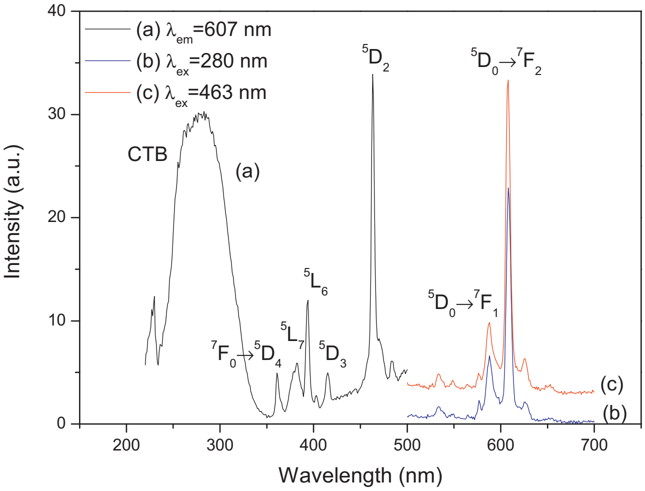

Fig. 2. Emission ($\lambda_{ex} = 280$, 463 nm) and excitation ($\lambda_{em} = 607$ nm) spectra of $Li_5(La_{2.70}Eu_{0.30})Nb_2O_{12}$ phosphor.

Fig. 2 shows representative emission spectra of $Li_5(La_{2.70}Eu_{0.30})Nb_2O_{12}$. The research of $Li_5La_3Nb_2O_{12}$ crystal structure indicated that the lanthanum atom is surrounded by four O atoms and forms a contracted tetrahedron [17]. It can be seen from Fig. 2 that the $^5D_0$–$^7F_2$ transition (electric dipole transition) is the dominant one, which reveals that Eu^{3+} ions are located in the asymmetry sites [18]. So we think that the doped Eu^{3+} ions should substitute the La^{3+} sites. The CIE (Commission Internationale de l'Eclairage) chromaticity coordinates are calculated to be $x = 0.53$ and $y = 0.45$. The excitation spectrum of the Eu^{3+} emission (607 nm) consists of well-known Eu^{3+} f–f transition lines and a broad band peak at about 280 nm. Usually, for the Eu^{3+}-doped samples, the position of charge transfer band (CTB) can be calculated with the help of an empirical formula given by Reisfeld and Jørgensen [19]

$$E_{ct}(\mathrm{cm}^{-1}) = [\chi_{opt}(\mathrm{X}) - \chi_{uncorr}(\mathrm{M})] \times 30{,}000\ \mathrm{cm}^{-1} \qquad (1)$$

where E_{ct} is the position of the CTB in cm^{-1}, $\chi_{opt}(X)$ is the optical electronegativity of the anion, and $\chi_{uncorr}(M)$ is that of the central metal ion. Using the Pauling scale for electronegativity, namely $\chi_{opt}(O) = 3.44$, and $\chi_{uncorr}(Eu^{3+}) = 1.74$ [20], the CTB of Eu–O can be estimated to be 51,000 cm^{-1} (196 nm). However, this calculated value shows large difference with the experimental data (280 nm). There are two possible reasons which can be applied to explain this red shift [21]. One is that in the Sc–Lu–Y–Gd–La series, the position of Eu–O CTB in La^{3+} host has minimum E_{ct}. Another is that in Eu^{3+} doped composite oxides (Eu–O–M, M is metal element), the energy of CTB depends not only on the coordination atom O, but also on the metal atom M. $Li_5La_3Nb_2O_{12}$ is a composite oxide. In this case, the electronegativity of Nb is small and this weakens the interaction between M and O, which is beneficial for transferring the electron from O to Eu and decreases the E_{ct}. In addition, the charge transfer transition of host, namely, an electron from an oxygen ligand to the empty 4*d* orbital of the central niobium atoms in NbO groups (Nb→O) could also happen in this region. In the crystal structure of $Li_5La_3Nb_2O_{12}$, Nb atom is surrounded by six oxygen atoms and forms NbO_6 octahedron. Many authors report that NbO_6 group has absorption band at about 300 nm [22–24]. So we regard that the 280 nm absorption band in the excitation spectrum could be attributed to the overlap of CTB of Eu–O and NbO_6 group absorption. The 463 nm excitation peak is strong and matches the emission of blue light emitting diode. So $Li_5La_3Nb_2O_{12}:Eu^{3+}$ could be a candidate phosphor for phosphor-converted white LEDs.

The concentration dependence of emission intensity of $^5D_0$–$^7F_2$ transition is shown in Fig. 3. It can be seen that the emission intensity increases with increasing Eu^{3+} concentration, and the optimum value of x in $Li_5(La_{3-x}Eu_x)Nb_2O_{12}$ is 0.30. The emission intensity shows similar trend when three different frequencies of excitation light are used (280, 393 and 463 nm). The high doping concentration of activated ions in a phosphor can suffer high power excitation in the application of solid state lighting, which is very useful for devices. Concentration quenching is due to migration of the excitation energy to trap sites [25]. Therefore, concentration quenching often takes place when the average distance between the Eu^{3+} ions is short enough to transfer their energy. So it is possible to estimate the critical distance (R_0, the distance at which the probability of transfer is equal to the probability of radiative emission) from the concentration quenching data. The critical transfer distance (R_0) can be derived roughly from the following formula proposed by Blasse [26]:

$$R_0 \approx 2 \times \left(\frac{3V}{4\pi x_c N}\right)^{1/3} \tag{2}$$

where x_c is the critical concentration at which the quenching occurs, N is the number of La^{3+} ions in the $Li_5La_3Nb_2O_{12}$ unit cell and V is the volume of the unit cell. By taking the experimental and analytical values of V, N and x_c (2095.68 Å^3, 8, 0.30, respectively), the critical transfer distance of Eu^{3+} in $Li_5La_3Nb_2O_{12}:Eu^{3+}$ phosphor is calculated to be 12 Å, which indicates that the mechanism of exchange interaction plays no role in energy transfer between Eu^{3+} ions in the $Li_5La_3Nb_2O_{12}:Eu^{3+}$ phosphors. In general, the exchange interaction is dominant only for short distance (typical critical distances of 5 Å). So the energy transfer in $Li_5La_3Nb_2O_{12}:Eu^{3+}$ will take place only through electric multipolar interaction.

The decay curves of the 610 nm luminescence of Eu^{3+} in $Li_5La_3Nb_2O_{12}:Eu^{3+}$ phosphors with different doped concentrations are shown in Fig. 4. It can be seen that all of the curves show exponential decay, and the heavier the doped concentration, the shorter the lifetime. The decay curves can be fitted by single exponential equation: $I(\mathrm{t})=I_0+A\ \exp(-t/\tau)$, where I and I_0 is the luminescence intensity, A is a constant, t is the time, τ is the decay time for the exponential components. The τ extracted from the fitted curve is 1.14 ms for $Li_5(La_{2.999}Eu_{0.001})Nb_2O_{12}$ and 0.37 ms for $Li_5(La_2Eu)Nb_2O_{12}$. When the doped concentration increases, the decrease in lifetime can be attributed to the non-radiative relaxation between Eu^{3+} ions. When the doped concentration increases, the sample has more and more quenching centers and the non-radiative rate increases, which causes the lifetime to be shortened [27].

The thermal quenching property of phosphor is one of the important issues to be considered in white LEDs especially in high-power devices. The temperature dependences of PL emission spectra of $Li_5(La_{2.70}Eu_{0.30})Nb_2O_{12}$ excited by 266 nm light are shown in Fig. 5. With increase in temperature, the thermal quenching takes places and the emission intensity decreases obviously. The thermal quenching is due to the thermal relaxation through the crossing point between the excited state and the ground state in the configurational coordinate diagram [18]. A non-radiative transition occurs because of the interaction between the electron and thermally active phonon [28].

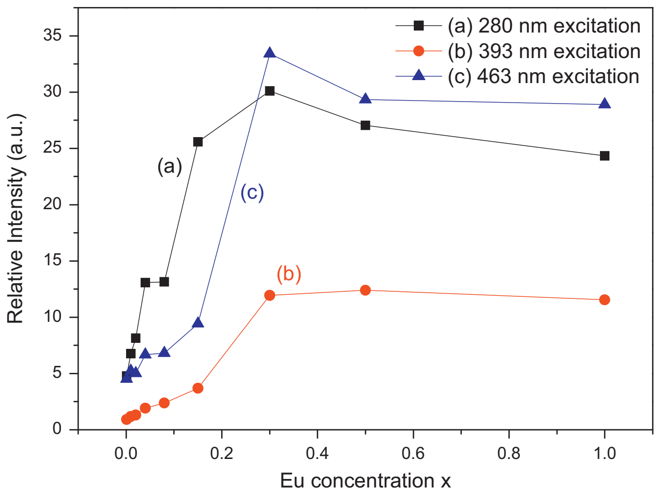

Fig. 3. Emission intensity of $^5D_0$–$^7F_2$ transition as a function of Eu^{3+} concentration for $Li_5La_3Nb_2O_{12}:Eu^{3+}$ under different excitation lights.

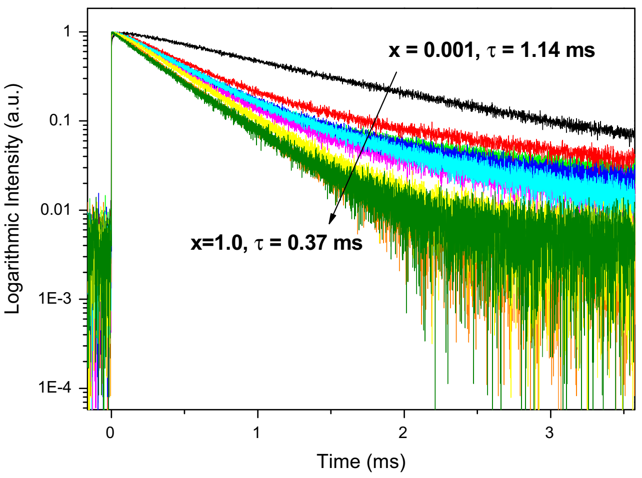

Fig. 4. Decay curves of the 610 nm luminescence of Eu^{3+} as a function of Eu^{3+} concentration in $Li_5La_3Nb_2O_{12}:Eu^{3+}$ phosphors excited at 266 nm.

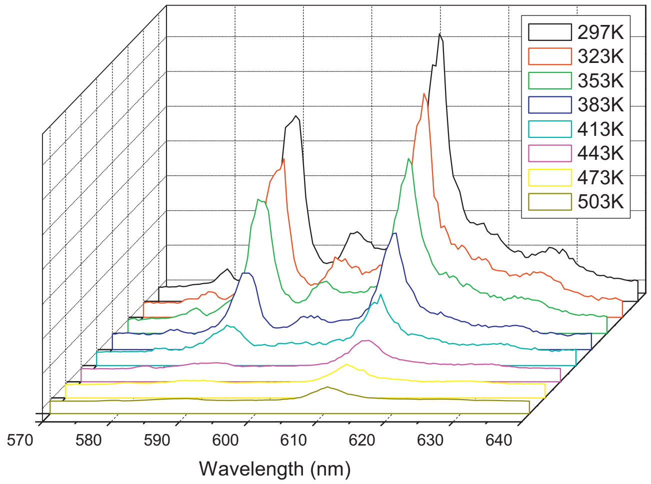

Fig. 5. Emission spectra of the Eu^{3+} as a function of temperature dependence for $Li_5(La_{2.70}Eu_{0.30})Nb_2O_{12}$.

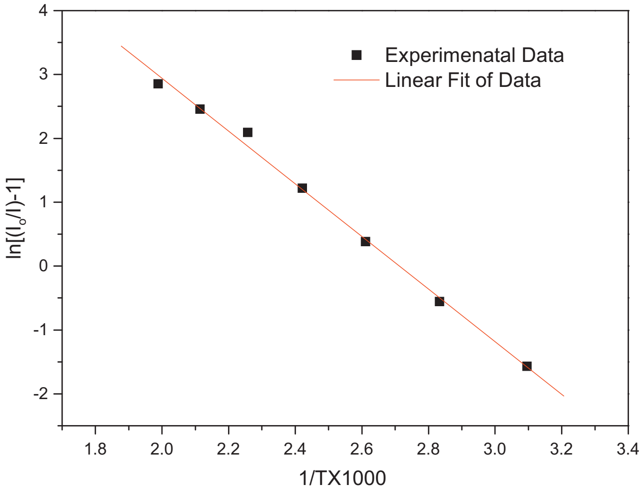

Fig. 6. Activation energy for thermal quenching of $Li_5(La_{2.70}Eu_{0.30})Nb_2O_{12}$.

The thermal activation energy for the thermal quenching of the Eu^{3+} emission was determined by measuring the temperature dependence of the Eu^{3+} emission intensity. The temperature dependence of the luminescence intensity is described by a modified Arrhenius equation [29]:

$$I(T) = \frac{I_0}{1 + c\,\exp\left(-E/kT\right)} \tag{3}$$

where I_0 is the initial intensity, $I(T)$ is the intensity at a given temperature T, c is a constant, E is the activation energy for thermal quenching and k is the Boltzmann constant. Fig. 6 plots ln $[(I_0/I)-1]$ vs. $1/T$. When performing linear fitting, the obtained value of slope is -4121. According to Eq. (2), the calculated activation energy is about 0.36 eV.

The decay curves of the Eu^{3+} emission (610 nm) as a function of temperature for $Li_5(La_{2.70}Eu_{0.30})Nb_2O_{12}$ phosphor excited at 266 nm are shown in Fig. 7. It is found that the lifetimes decrease from 0.54 ms at room temperature to 0.39 ms at 503 K. The reason is that the lifetime of excited states decreases with increase in temperature, and then resulting in a substantial increase in non-radiative relaxation rate (the radiative relaxation rate usually also increases slightly) [30].

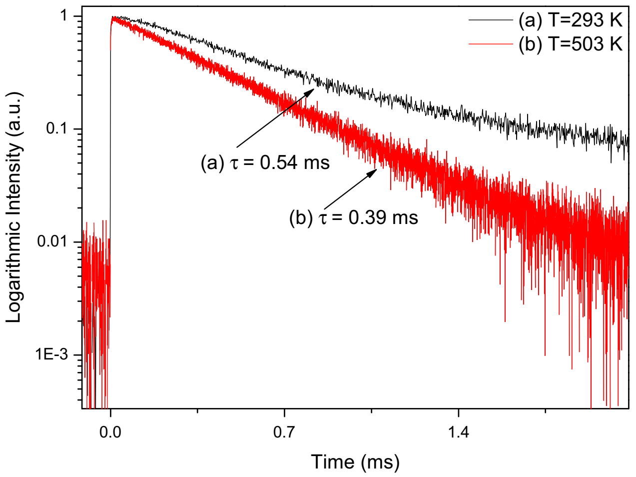

Fig. 7. Decay curves of the Eu^{3+} emission (610 nm) as a function of temperature for $Li_5(La_{2.70}Eu_{0.30})Nb_2O_{12}$ phosphor excited at 266 nm.

4. Conclusions

$Li_5(La_{3-x}Eu_x)Nb_2O_{12}$ phosphors were prepared by solid state reaction. XRD patterns reveal that the samples are of single phase when $x \leq 1.0$. All the samples show red luminescence. The $^5D_0$–$^7F_2$ transition is the dominant one indicating that the Eu^{3+} ion occupies a site with a deviation from inversion symmetry. The CIE chromaticity coordinates are $x=0.53$ and $y=0.45$. The optimum concentration of Eu^{3+} ions is 0.30. The critical transfer distance of Eu^{3+} in $Li_5La_3Nb_2O_{12}$:Eu^{3+} phosphor is about 12 Å. The excitation spectrum consists of a strong Eu^{3+} f–f excitation peak at 463 nm and a broad band peak at about 280 nm. The decay curves show single exponential decay and that the lifetimes become shorter with increasing Eu^{3+} concentration. The decrease in lifetime can be attributed to the non-radiative relaxation between Eu^{3+} ions. At high temperature, the thermal quenching takes places and the emission intensity decreases obviously. The thermal quenching can be explained with configurational coordinate diagram. The lifetimes also decrease at high temperature because of a substantial increase in non-radiative relaxation rate.

Acknowledgments

The project was sponsored by SRF for ROCS, SEM (2011-508), Technology Program of Hunan Provincial Department of Housing and Urban-Rural development (No. 201020), the Science and Technology Program of Hunan Province (No. 2011GK3223) and Geology Exploration program of Hunan Provincial Department of Land and Resources.

References

[1] J. Thakur, D.P. Dutta, H. Bagla, A.K. Tyagi, Effect of host structure and concentration on the luminescence of Eu^{3+} and Tb^{3+} in borate phosphors, Journal of the American Ceramic Society 95 (2012) 696–704.

[2] K. Mishra, S.K. Singh, A.K. Singh, S.B. Rai, Optical characteristics and charge transfer band excitation of Dy^{3+} doped Y_2O_3 phosphor, Materials Research Bulletin 47 (2012) 1339–1344.

[3] E. Çırçır, N. Ozpozan Kalaycioglu, Host-sensitized phosphorescence of Mn^{4+}, $Pr^{3+,4+}$ and Nd^{3+} in $MgAl_2Si_2O_8$, Materials Research Bulletin 47 (2012) 1138–1141.

[4] Y.-C. Chen, W.-Y. Huang, T.-M. Chen, Enhancing the performance of photovoltaic cells by using down-converting $KCaGd(PO_4)_2$:Eu^{3+} phosphors, Journal of Rare Earths 29 (2011) 907–910.

[5] X.-M. Zhang, W.-L. Li, K.H. Jang, H.J. Seo, Luminescence enhancement by energy transfer from Ce^{3+} ions in $Ba_{1.6}Ca_{0.4}P_2O_7$:Ce^{3+}:Tb^{3+} phosphor, Current Applied Physics 12 (2012) 299–302.

[6] F.-G. Meng, X.-M. Zhang, H.J. Seo, Optical properties of Sm^{3+} and Dy^{3+} ions in $Gd_2MoB_2O_9$ host lattice, Optics and Laser Technology 44 (2012) 185–189.

[7] F. Meng, X. Zhang, W. Li, T. Xie, H.J. Seo, Luminescence and time-resolved spectroscopy properties of $(Gd_{1-x}Eu_x)(BO_2)_3$ multicrystals, The Journal of Physics and Chemistry of Solids 73 (2012) 564–567.

[8] Q. Zhang, Q. Meng, Y. Tian, X. Feng, J. Sun, S. LÜ, Luminescent properties of Eu^{3+} doped Gd_2WO_6 and $Gd_2(WO_4)_3$ nanophosphors prepared via co-precipitation method, Journal of Rare Earths 29 (2011) 815–821.

[9] H. Wu, X.M. Zhang, C.F. Guo, R. Xu, M.M. Wu, Q. Su, Three-band white light from InGaN-based blue LED chip precoated with green/red phosphors, IEEE Photonics Technology Letters 17 (2005) 1160–1162.

[10] Y.Q. Li, N. Hirosaki, R.J. Xie, T. Takeda, M. Mitomo, Yellow-orange-emitting $CaAlSiN_3$:Ce^{3+} phosphor: structure, photoluminescence, and application in white LEDs, Chemistry of Materials 20 (2008) 6704–6714.

[11] R.-J. Xie, N. Hirosaki, T. Suehiro, F.-F. Xu, M. Mitomo, A simple, efficient synthetic route to $Sr_2Si_5N_8$:Eu^{2+}-based red phosphors for white light-emitting diodes, Chemistry of Materials 18 (2006) 5578–5583.

[12] A. Katelnikovas, J. Plewa, D. Dutczak, S. Möller, D. Enseling, H. Winkler, A. Kareiva, T. Jüstel, Synthesis and optical properties of green emitting garnet phosphors for phosphor-converted light emitting diodes, Optical Materials 34 (2012) 1195–1201.

[13] L.H.C. Andrade, S.M. Lima, M.L. Baesso, A. Novatski, J.H. Rohling, Y. Guyot, G. Boulon, Tunable light emission and similarities with garnet structure of Ce-doped LSCAS glass for white-light devices, Journal of Alloys and Compounds 510 (2012) 54–59.

[14] J. Wiehl, S. Kemmler-Sack, Cathodo- and photoluminescence in the Eu^{3+} activated garnets of type $Y_{3-x}Ln_xTe_2Li_3O_{12}$ (Ln = Lu, La) and $Gd_{3-x}La_xTe_2Li_3O_{12}$, Physica Status Solidi A 104 (1987) 863–872.

[15] S. Zhang, Y. Huang, L. Shi, X. Qiao, H.J. Seo, Synthesis, luminescence and crystallographic structure of Eu^{3+}-doped garnet-type yafsoanite $Ca_3Te_2(ZnO_4)_3$, Physica B: Condensed Matter 404 (2009) 4136–4141.

[16] Y.H. Song, T.Y. Choi, T. Masaki, K. Senthil, D.H. Yoon, Photoluminescence properties and synthesis of nano-sized YAG: Ce^{3+} phosphor via novel synthesis method, Current Applied Physics 12 (2012) 479–482.

[17] H. Hyooma, K. Hayashi, Crystal structures of $La_3Li_5M_2O_{12}$ (M = Nb, Ta), Materials Research Bulletin 23 (1988) 1399–1407.

[18] G. Blasse, B.C. Grabmaier, Luminescent Materials, Springer, Berlin, 1994.

[19] R. Reisfeld, C.K. Jørgensen, in: Lasers and Excited States of Rare Earths, Springer-Verlag, Berlin, 1977.

[20] Q. Su, in: Chemistry of Rare Earths, Henan Science and Technology Press, Henan, 1993 (in Chinese).

[21] Q. Su, in: Q. Su (Ed.), Rare Earths Spectroscopy, World Scientific, Singapore, 1990, pp. 214.

[22] Y.J. Hsiao, T.H. Fang, Y.S. Chang, Y.H. Chang, C.H. Liu, L.W. Ji, W.Y. Jywe, Structure and luminescent properties of $LaNbO_4$ synthesized by sol–gel process, Journal of Luminescence 126 (2007) 866–870.

[23] S.A. Naidu, S. Boudin, U.V. Varadaraju, B. Raveau, A crystal chemical approach to tuning of emission properties in rare earth doped ternary niobates, Journal of Materials Chemistry 22 (2012) 1088–1093.

[24] J. Huang, L. Zhou, Z. Liang, F. Gong, J. Han, R. Wang, Promising red phosphors $LaNbO_4$:Eu^{3+}, Bi^{3+} for LED solid-state lighting application, Journal of Rare Earths 28 (2010) 356–360.

[25] G. Blasse, Energy-transfer between inequivalent Eu^{2+} ions, Journal of Solid State Chemistry 62 (1986) 207–211.

[26] G. Blasse, Energy transfer in oxidic phosphors, Philips Research Reports 24 (1969) 131–144.

[27] T.H. Fang, Y.J. Hsiao, Y.S. Chang, Y.H. Chang, Photoluminescent characterization of $KNbO_3$:Eu^3, Materials Chemistry and Physics 100 (2006) 418–422.

[28] J.S. Kim, Y.H. Park, S.M. Kim, J.C. Choi, H.L. Park, Temperature-dependent emission spectra of M_2SiO_4: Eu^{2+} (M = Ca, Sr, Ba) phosphors for green and greenish white LEDs, Solid State Communications 133 (2005) 445–448.

[29] I. Baginskiy, R.S. Liu, Significant improved luminescence intensity of Eu-doped CaSiOCl green phosphor for white LEDs synthesized through two-stage method, Journal of the Electrochemical Society 156 (2009) G29–G32.

[30] A. Meijerink, G. Blasse, Luminescence and temperature-dependent decay behavior of dibalent europium in $Ba_5SiO_4Cl_6$, $Ba_5SiO_4Br_6$, Journal of Luminescence 47 (1990) 1–5.